# Dynamics of Fourier domain mode-locked lasers

**S. Slepneva,[1,2] B. Kelleher,[1,2,*] B. O'Shaughnessy,[1,2] S.P. Hegarty,[1] A.G. Vladimirov,[1,2,3] and G. Huyet[1,2]**

[1] *Tyndall National Institute, University College Cork, Lee Maltings, Dyke Parade, Cork, Ireland*

[2] *Centre for Advanced Photonics and Process Analysis, Cork Institute of Technology, Cork, Ireland*

[3] *Weierstrass Institute for Applied Analysis and Stochastics, Mohrenstrasse 39, D-10117 Berlin, Germany*

[*] *bryan.kelleher@tyndall.ie*

**Abstract:** An analysis of the dynamical features in the output of a Fourier Domain Mode Locked laser is presented. An experimental study of the wavelength sweep-direction asymmetry in the output of such devices is undertaken. A mathematical model based on a set of delay differential equations is developed and shown to agree well with experiment.



**OCIS codes:** (140.3600) Lasers, tunable; (140.3430) Laser theory; (110.4500) Optical coherence tomography.

## References and links

1. R. Huber, M. Wojtkowski, K. Taira, J. Fujimoto, and K. Hsu, "Amplified, frequency swept lasers for frequency domain reflectometry and OCT imaging: design and scaling principles," Opt. Express **13**, 3513–3528 (2005).
2. R. Huber, M. Wojtkowski, and J. G. Fujimoto, "Fourier domain mmode locking (FDML): a new laser operating regime and applications for optical coherence tomography," Opt. Express **14**, 3225–3237 (2006).
3. A.F. Fercher, W. Drexler, C.K. Hitzenberger and T. Lasser, "Optical coherence tomography - principles and applications," Rep. Prog. Phys. **66**, 239–303 (2003).
4. B. R. Biedermann, W. Wieser, C. M. Eigenwillig, T. Klein, and R. Huber, "Direct measurement of the instantaneous linewidth of rapidly wavelength-swept lasers," Opt. Lett. **35**, 3733–3735 (2010).
5. S. Todor, B. Biedermann, W. Wieser, R. Huber, and C. Jirauschek, "Instantaneous lineshape analysis of Fourier domain mode-locked lasers," Opt. Express **19**, 8802–8807 (2011).
6. S. Todor, B. Biedermann, R. Huber, and C. Jirauschek, "Balance of physical effects causing stationary operation of fourier domain mode-locked lasers," J. Opt. Soc. Am B **29**, 656–664 (2012).
7. R. Huber, D. C. Adler, and J. G. Fujimoto, "Buffered Fourier domain mode locking: unidirectional swept laser sources for optical coherence tomography imaging at 370,000 lines/s," Opt. Lett. **31**, 2975–2977 (2006).
8. M. Y. Jeon, J. Zhang, and Z. Chen, "Characterization of Fourier domain modelocked wavelength swept laser for optical coherence tomography imaging," Opt. Express **16**, 3727–3737 (2008).
9. A. Bilenca, S. H. Yun, G. J. Tearney, and B. Bouma, "Numerical study of wavelength-swept semiconductor ring lasers: the role of refractive-index nonlinearities in semiconductor optical amplifiers and implications for biomedical imaging applications," Opt. Lett. **31**, 760–762 (2006).
10. C. Jirauschek, B. Biedermann, and R. Huber, "A theoretical description of Fourier domain mode locked lasers," Opt. Express **17**, 24013–24019 (2009).
11. S. Todor, B. Biedermann, R. Huber, and C. Jirauschek, "Analysis of the optical dynamics in fourier domain mode-locked lasers," in Advanced Photonics & Renewable Energy, OSA Technical Digest (CD) (Optical Society of America, 2010), p. SWC4.
12. D. C. Adler, W. Wieser, F. Trepanier, J. M. Schmitt, and R. A. Huber, "Extended coherence length Fourier domain mode locked lasers at 1310 nm," Opt. Express **19**, 20930–20939 (2011).
13. W. Wieser, T. Klein, D. C. Adler, F. Trépanier, C. M. Eigenwillig, S. Karpf, J. M. Schmitt, and R. Huber, "Extended coherence length megahertz FDML and its application for anterior segment imaging," Biomed. Opt. Express **3**, 2647–2657 (2012).

#189874 - $15.00 USD Received 7 May 2013; revised 27 Jun 2013; accepted 27 Jun 2013; published 6 Aug 2013

14. A. G. Vladimirov and D. Turaev, "Model for passive mode-locking in semiconductor lasers," Phys. Rev. A **72**, 033808 (2005).
15. A. Vladimirov, D. Turaev, and G. Kozyreff, "Delay differential equations for mode-locked semiconductor lasers," Opt. Lett. **29**, 1221–1223 (2004).
16. A. Vladimirov and D. Turaev, "A new model for a mode-locked semiconductor laser," Radiophys. and Quantum Electronics **47**, 769–776 (2004).
17. S. Kashchenko, "Normalization techniques as applied to the investigation of dynamics of difference-differential equations with a small parameter multiplying the derivative," Differ. Uravn. **25**, 1448–1451 (1989).
18. G. Giacomelli and A. Politi, "Multiple scale analysis of delayed dynamical systems," Physica D **117**, 26–42 (1998).
19. S. Yanchuk and M. Wolfrum, "A multiple timescale approach to the stability of external cavity modes in the lang-kobayashi system using the limit of large delay," SIAM J. Appl. Dyn. Syst. **9**, 519–535 (2010).
20. M. Lichtner, M. Wolfrum, and S. Yanchuk, "The spectrum of delay differential equations with large delay," SIAM J. Math. Anal. **43**, 788–802 (2011).

## 1. Introduction

Frequency swept sources have greatly improved the acquisition speed and sensitivity of optical coherence tomography (OCT). The cavities of swept sources designed as fiber ring lasers include two basic components: a gain element (typically a semiconductor optical amplifier (SOA)) and a fast tunable filter. The tuning rate of the filter and the time required for building up the lasing action from spontaneous emission mostly define the maximum achievable sweep rate. Isolators are also typically included in the cavity to ensure unidirectional circulation of the light. Conventional swept laser sources can have cavity lengths of several meters that act to limit the sweep rate while maintaining efficient lasing [1]. By incorporating an optical delay so that the cavity roundtrip matches the tuning period of the filter, the laser can be made to operate in the so-called Fourier Domain Mode Locked (FDML) regime [2]. This is characterized by high efficiency and more coherent lasing due to the fact that the lasing does not have to continually restart from amplified spontaneous emission and the whole sweep is stored in the cavity. The length of the FDML laser cavity is thus necessarily in the range of several kilometers to match filter sweep rates of tens of kHz. Other sources used in OCT include superluminescent diodes, Kerr-lens mode locked lasers and supercontinuum sources (see [3] and references within).

The excellent performance demonstrated by FDML lasers as light sources for OCT has motivated both experimental and theoretical studies of the laser properties. For example, an experimental approach for linewidth measurement is presented in [4] where a fast synchronous time gating method reveals a linewidth of several GHz while theoretical research has primarily focused on defining the influence of different cavity components and the physical effects governing the laser performance [5, 6].

Studies of swept source intensity outputs have revealed an asymmetry in the output intensity within one period of the modulation between the forward filter sweep (the filter moving from shorter to longer wavelengths) and the backward filter sweep (the filter moving from longer to shorter wavelengths). For a conventional swept source a significantly lower intensity was observed in the backward sweep compared to that observed in the forward sweep [1]. This power drop [7, 8] as well as a linewidth asymmetry in the forward and backward sweeps of the laser were observed for FDML lasers in [6]. Theoretical descriptions have relied on the study of partial differential equations describing the propagation in optical fiber and these have confirmed that the interplay of SOA nonlinearity and the direction of the sweep is responsible for the observed asymmetry in both long and intermediate laser cavities [8–11]. This property is crucial for OCT applications as only one direction of the sweep can thus be used for the imaging system. With modifications of FDML lasers such as the application of a buffering technique [7], the introduction of broadband dispersion compensation in the cavity [12] and SOA modulation [13], current FDML OCT systems operate with a sweep rate in MHz range.

#189874 - $15.00 USD Received 7 May 2013; revised 27 Jun 2013; accepted 27 Jun 2013; published 6 Aug 2013

Typically the filter tuning frequency is slightly detuned from the roundtrip time. We define the detuning as $f_{\text{filter}} - \frac{1}{T}$ where $f_{\text{filter}}$ is the sweep rate of the filter and $T$ is the roundtrip time. The detuning affects some aspects of the FDML laser performance such as the number of roundtrip times required for the FDML to operate in a stationary regime after self starting [10]. Also, the sweep direction asymmetry in the intensity traces is reversed when the detuning is changed from positive to negative [10].

Here, we describe the dynamics of an FDML both experimentally and theoretically using a delay differential equation model. We study the laser output as a function of the detuning and show that the asymmetry in the output has a fundamental origin related to the field-matter interactions in the laser. One half of the sweep consists of jumps between stable modes while the other consists of a complex oscillating output. We explain the source of this asymmetry and show that it arises generically in the swept ring laser source geometry by examining FDML, quasistatic and conventional swept-source regimes.

## 2. Experimental setup

In the experimental setup we used a standard configuration of an FDML laser as presented in Fig. 1. The gain medium was provided by a semiconductor optical amplifier (SOA) (Thorlabs, BOA 1132) with 32.1 dB small signal gain, 16.9 dBm saturation output power and 88.1 nm optical 3 dB bandwidth. The amplified spontaneous emission peak wavelength was 1303.8 nm. The SOA had two incorporated isolators. The wavelength selective element in the cavity was a fiber Fabry-Pérot tunable narrow band (50 pm) optical bandpass filter (MicronOptics) with about 20 THz free spectral range and 1.3 dB insertion loss. Fiber optical isolators with 42 dB peak isolation were placed before and after the filter to avoid parasitic back reflections. The laser power was optimized with a polarization controller. The total length of the cavity was about 20 km with most of this from a long SMF-28 optical fiber delay. The filter was tuned with an Agilent 33500 Series 30 MHz waveform generator. The frequency corresponding to the round trip in the ring cavity was 10,175.687 Hz. A 50/50 beam splitter was used as an output tap coupler. An optical spectrum analyzer, a DC-coupled broadband 12 GHz photoreciever (Newport, 1554-B) and a real time oscilloscope of 12 GHz bandwidth were used to analyze the laser output.

## 3. Experimental results

### *3.1. FDML swept source regime*

In order to investigate the emitted signal in real time the output of the laser was connected to a fast optical detector and the signal analyzed using a real-time oscilloscope with 12 GHz bandwidth. The tuning range of the filter was varied between 0.5 nm and 12 nm. A typical output optical spectrum is presented in Fig. 2.

As previously reported, the detuning strongly influences the laser output. The intensity within one roundtrip time for positive detuning is shown in Fig. 3(a) and for negative detuning in Fig. 3(b). In both cases the magnitude of the detuning was approximately 15 mHz. The tuning voltage is shown above the intensity in red, and the turning point of the sweep is approximately at 0 $\mu$s indicating the moment when the sweep changes from decreasing wavelength to increasing wavelength. An obvious qualitative change in the laser output is observed close to the turning point for both cases. For the positive detuning and forward wavelength sweep case, the output resembled a series of jumps from one stable output to another while the backward wavelength sweep resulted in complex GHz oscillations, as shown in the inset. For the negative detuning case the situation was reversed.

As the sweeping range was varied the same qualitative dependence on the detuning was ob-

#189874 - $15.00 USD Received 7 May 2013; revised 27 Jun 2013; accepted 27 Jun 2013; published 6 Aug 2013

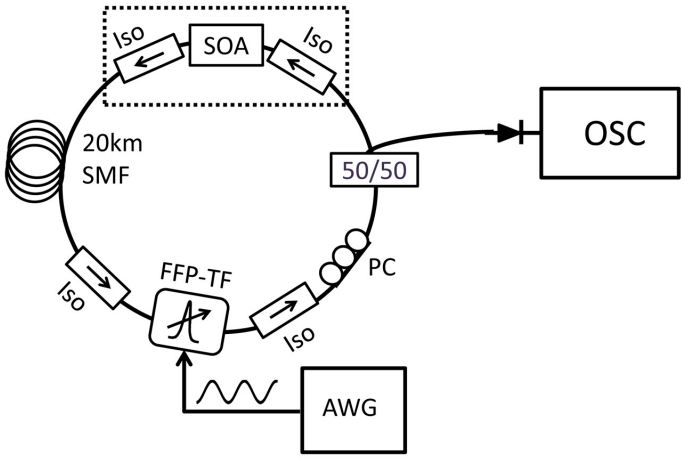


Fig. 1. Experimental set-up of the ring laser. Iso: Isolator. FFP-TF: Fiber Fabry-Pérot Tunable Filter. AWG: Arbitrary Waveform Generator. SOA: Semiconductor Optical Amplifier. OSC: Oscilloscope. SMF: Single Mode Fiber. PC: Polarization Controller.

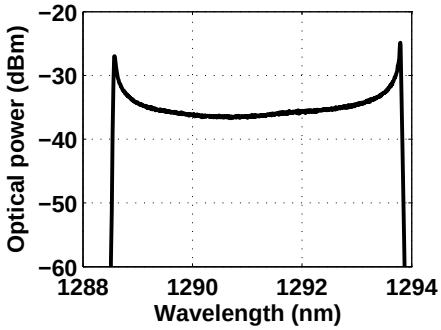


Fig. 2. Example of optical spectrum in FDML regime.

served while the number of dropouts decreased as the span was made smaller. By varying the central frequency of the filter through the range 1297 nm to 1342 nm (centred approximately on the minimum dispersion position) while keeping the sweeping range the same, it was possible to investigate the influence of chromatic dispersion. For sufficient detunings the qualitative properties of the laser intensity remained unchanged in this range demonstrating that the dispersion played a weak role, if any, in the genesis of the observed asymmetry. Nonetheless, while it is not the phenomenon responsible for the asymmetry, it is possible to observe some complicating effects resulting from dispersion for extremely low detunings but we do not pursue these in this work.

### *3.2. Quasistatic regimes*

Physically a perfectly synchronous FDML regime and a static filter regime should be related by a simple change of reference frame (and this intuitive idea is expressed formally below in Section 4.1). Thus one might expect a quasistatic regime where the filter tuning frequency is

#189874 - $15.00 USD Received 7 May 2013; revised 27 Jun 2013; accepted 27 Jun 2013; published 6 Aug 2013

kept extremely low (100 mHz) to be similarly related to the slightly detuned FDML regime and one should expect to see the same dynamics in both cases. This is indeed the case and the same asymmetry was observed with pronounced dropouts in the forward direction of the sweep and a complex signal for the backward direction of the sweep as shown in Fig. 4.

To consider the effect of cavity length, such as losses, dispersion and its sensitivity to environmental temperature fluctuations,we now consider a conventional swept source regime where the 20 km fiber delay is removed from the cavity leaving a cavity length of about 17 m. The filter tuning frequency was 100 mHz again and the same behavior was observed with the dropouts between stable outputs for the increasing wavelength part of the sweep and complex oscillations for the decreasing part. Thus the phenomenon appears to be generic for the geometry of the system.

## 4. Theory

### *4.1. Model equations and CW solutions*

To model the FDML laser theoretically we use a delay differential equation model similar to that used to describe passively mode locked lasers in [14–16] but without the equation for saturable absorption. It is given by a set of two differential equations with time delay

$$\partial_t A + A - i\Delta(t)A = \sqrt{\kappa}e^{(1-i\alpha)G(t-T)/2}A(t-T), \tag{1}$$

$$\partial_t G = \gamma\left[g_0 - G - \left(e^G - 1\right)|A|^2\right], \tag{2}$$

where $A(t)$ is the electric field envelope at the entrance of the SOA and the carrier density is modeled via a saturable gain $G(t)$. The position of the central frequency of the spectral filter is defined by the time dependent quantity $\Delta(t) = r\sin(\Omega t)$, where the amplitude $r$ and frequency $\Omega$ of the sweep are normalized to the filter bandwidth $\Gamma$. The time variable $t$ is normalized to the inverse filter bandwidth $\Gamma^{-1}$. For simplicity the gain bandwidth is assumed to be infinitely wide. The parameters $\kappa$ and $\alpha$ are the linear attenuation factor per cavity round trip and the linewidth enhancement factor respectively and $g_0$ and $\gamma$ are the linear unsaturated gain parameter and normalized gain relaxation rate in the SOA, respectively. The normalized delay time is $T \gg 1$. Since, as mentioned above, the qualitative properties of the laser intensity time traces remain unchanged for different central wavelengths of the spectrum, we ignore chromatic dispersion

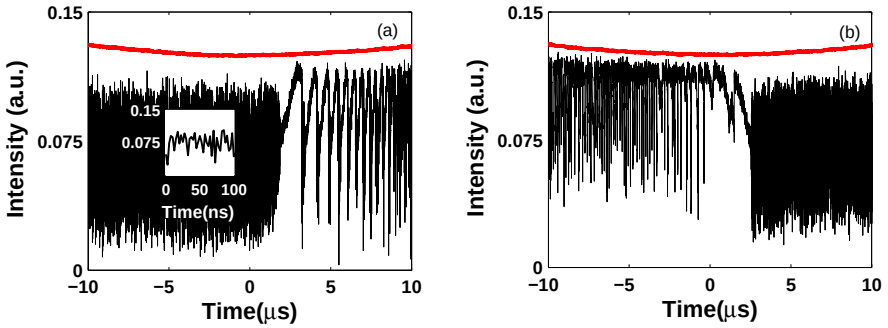


Fig. 3. Intensity as measured on the oscilloscope for (a) a detuning of +15mHz and (b) a detuning of -15mHz. The sweeping voltage of the filter is shown (in red) above the filter. The turning point of the sweep is approximately at 0 $\mu$s and the central wavelength of the filter is decreasing on the left and increasing on the right. The asymmetry has clearly reversed with the change of sign of the detuning.

#189874 - $15.00 USD Received 7 May 2013; revised 27 Jun 2013; accepted 27 Jun 2013; published 6 Aug 2013

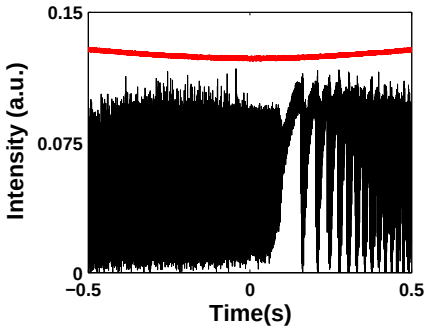


Fig. 4. Intensity as measured on the oscilloscope in a quasistatic regime. The filter sweep frequency was 100 mHz. The sweeping voltage of the filter is shown (in red) above the intensity. The turning point of the sweep is at 0 s and the central wavelength of the filter is decreasing on the left and increasing on the right.

together with some other phenomena such as the Kerr nonlinearity in the fiber delay line, and show that this minimal model is sufficient to understand the dynamics of the system.

Let us consider a static filter and the consequent CW solutions of Eqs. (1) and (2) with constant laser intensity and gain, $A = A_0 e^{i\omega t}$ and $G = G_0$. Substituting these into Eqs. (1) and (2) we get the following three equations for the modal amplitude $A_0$, frequency $\omega$, and saturated gain $G_0$:

$$1 = \sqrt{\kappa} e^{G_0/2} \cos\theta, \quad \Delta - \omega = \sqrt{\kappa} e^{G_0/2} \sin\theta, \quad g_0 - G_0 = (e^{G_0} - 1)R, \tag{3}$$

where $R = |A_0|^2$ and $\theta = \frac{\alpha G_0}{2} + \omega T$. The first two of these equations can be rewritten in the form

$$1 + (\Delta - \omega)^2 = \kappa e^{G_0}, \quad \Delta - \omega = \tan\left(\frac{\alpha G_0}{2} + T\omega\right).$$

Eqs. (3) have multiple solutions corresponding to longitudinal laser modes, which can be numbered by an index $n$. The intensities of these modes are given by

$$R_n = \frac{\kappa\left[g_0 - \ln\left(\frac{1+(\Delta-\omega_n)^2}{\kappa}\right)\right]}{1 - \kappa + (\Delta - \omega_n)^2} \tag{4}$$

with the frequencies $\omega_n$ obeying the transcendental equation

$$\omega_n = \Delta - \tan\left[\omega_n T + \frac{\alpha}{2}\ln\left(\frac{1 + (\Delta - \omega_n)^2}{\kappa}\right)\right]. \tag{5}$$

Figure 5 shows a typical example of a CW solution.

Besides this static filter regime we will consider several others, all of which are defined through $\Delta(t)$. First let us change the reference frame to one comoving with the filter. This is achieved with the transformation

$$A(t) = a(t) e^{i\int_0^t \Delta(\tau) d\tau}. \tag{6}$$

Substituting this into Eq. (1) yields:

$$\partial_t a + a = \sqrt{\kappa} e^{(1-i\alpha)G(t-T)/2 - i\int_{t-T}^{t}\Delta(\tau)d\tau} a(t-T).$$

#189874 - $15.00 USD Received 7 May 2013; revised 27 Jun 2013; accepted 27 Jun 2013; published 6 Aug 2013

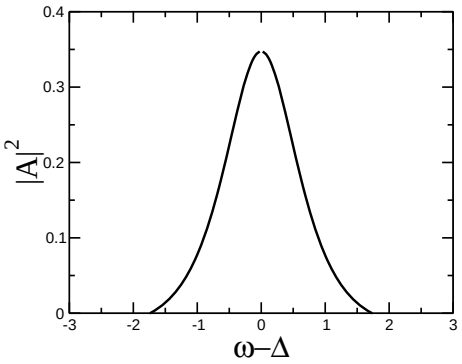


Fig. 5. Intensity of a CW solution of the model Eqs. (1) and (2) as a function of $\omega - \Delta$. In the limit $T \to \infty$ (or $\alpha \to 0$) it is symmetric with respect to $\omega = \Delta$. The parameter values are $\gamma = 0.1$, $\kappa = 0.2$, $\alpha = 2.0$ and $T \gg 1$.

Now let us consider the FDML regime where the filter is swept with a period exactly equal to the cavity round-trip time. In this case $\Delta(t) = r\sin(\Omega t)$ with $\Omega = 2\pi/T$. With this choice for $\Delta(t)$ and performing the integration in the exponential the system becomes autonomous:

$$\partial_t a + a = \sqrt{\kappa} e^{(1-i\alpha)G(t-T)/2} a(t-T),$$

$$\partial_t G = \gamma \left[ g_0 - G - \left(e^G - 1\right) |a|^2 \right].$$

This is identical in form to the system with a static filter centered at $\Delta = 0$. The CW solutions have the same form as those of Eqs. (1) and (2), $a(t) = a_n e^{i\omega_n t}$, in the comoving frame. However, unlike the CW solutions that appear in the genuine absence of a frequency sweep corresponding to the usual cavity longitudinal laser modes, these solutions are "FDML modes" since in the lab frame they correspond to the chirped frequency swept solutions

$$A(t) = a_n e^{i\omega_n t + i\int_0^t \Delta(\tau) d\tau}, \tag{7}$$

where $|a_n|^2 = R_n$ and $\omega_n$ are defined by Eqs. (4) and (5). This is the formal demonstration of the earlier intuitive idea of the equivalence of the static and exactly synchronous FDML operations.

Let us now consider the quasistatic case where $\Delta(t) = r\sin(\varepsilon t)$ with $\varepsilon \ll 2\pi/T$. Following the above steps we find

$$\partial_t a + a = \sqrt{\kappa} e^{(1-i\alpha)G(t-T)/2 + i\psi(t)} a(t-T), \tag{8}$$

with $\psi(t) = rT\sin(\varepsilon t)$ and $d\psi(t)/dt = O(\varepsilon)$, where we have used $\sin(\varepsilon T) \approx \varepsilon T$. One might expect that this should be formally equivalent to slightly detuned FDML operation. To test this we consider a period of modulation close to the cavity round trip time, $\Delta(t) = r\sin(\Omega t)$ with $\Omega = 2\pi/T + \varepsilon$ and $\varepsilon \ll \Omega$. Following the same steps and using the same relation $\sin(\varepsilon T) \approx \varepsilon T$ as above we get the same Eq. (8) but with

$$\psi(t) = rT\frac{\varepsilon}{\Omega}\sin(\Omega t). \tag{9}$$

Here, as before the phase $\psi$ is a slowly varying function of time, $d\psi(t)/dt = O(\varepsilon)$. The difference however is that while in the quasistatic case the results of our stability analysis will concern the usual CW longitudinal modes $A_n e^{i\omega_n t}$, in the case of slightly detuned FDML operation these results will be applied to the chirped modes.

#189874 - $15.00 USD Received 7 May 2013; revised 27 Jun 2013; accepted 27 Jun 2013; published 6 Aug 2013

*4.2. Stability of CW solutions and numerical results*

We consider now the stability of the CW solutions (4) and (5) in the quasistatic regime where the sweep frequency is changed very slowly in time, $\Omega \ll 2\pi/T$.

When the central frequency of the filter is fixed only those CW solutions are stable for which $|\omega - \Delta|$ is sufficiently small. Therefore, when the filter frequency is swept adiabatically, transitions between different groups of modes should take place. To study these transitions in more detail let us consider the stability of the CW solutions (4) and (5). The system (1) and (2) linearized at a CW solution given by $R, \omega$ and $G_0$ from Eq. 3 can be represented as

$$\partial_t \vec{x} = \mathscr{A}\vec{x} + \mathscr{B}\vec{x}(t-T),$$

where

$$\vec{x} = \begin{pmatrix} \mathrm{ReA} \\ \mathrm{ImA} \\ \mathrm{G} \end{pmatrix},$$

$$\mathscr{A} = \begin{pmatrix} -1 & \omega-\Delta & 0 \\ \Delta-\omega & -1 & 0 \\ -2\gamma(e^{G_0}-1)\sqrt{R} & 0 & -\gamma(1+e^{G_0}R) \end{pmatrix},$$

and

$$\mathscr{B} = \begin{pmatrix} 1 & \Delta-\omega & \frac{\sqrt{R}}{2}(1+\alpha\omega-\alpha\Delta) \\ \omega-\Delta & 1 & -\frac{\sqrt{R}}{2}(\alpha+\Delta-\omega) \\ 0 & 0 & 0 \end{pmatrix}.$$

The characteristic equation is

$$\det\left(-\lambda I + \mathscr{A} + \mathscr{B}e^{-\lambda T}\right) = 0,$$

where $I$ is the identity matrix. Following [17–20] we decompose the solutions of the characteristic equation into two parts with different scaling properties in $T$. These are the so-called pseudocontinuous spectrum which scales as $Re(\lambda) \sim 1/T$ and the strongly stable (unstable) spectrum which scales as $Re(\lambda) \sim 1$ for large $T$ [20]. The pseudocontinuous part is found as follows. We can write $\lambda$ as a series of terms of increasing powers of $1/T$. To first order we have

$$\lambda = i\nu_0 + \frac{\mu_1 + i\nu_1}{T}$$

for real $\nu_0$, $\mu_1$ and $\nu_1$. Then the characteristic equation can be represented in the form

$$\det\left(\mathscr{A} - i\nu_0 I + Y\mathscr{B}\right) = 0,$$

and so

$$\begin{aligned} &\left[\gamma(1+e^{G_0}R) + i\nu_0\right]\left[(Y-1)^2(\Delta-\omega)^2 + (Y-1-i\nu_0)^2\right] \\ &= \gamma RY(e^{G_0}-1)\left[(Y-1)\left(1+(\Delta-\omega)^2\right) + i\nu_0(\alpha(\Delta-\omega)-1)\right], \end{aligned} \tag{10}$$

where $Y = e^{-(\mu_1+i\nu_1)-i\nu_0 T}$. Therefore, the real parts of the eigenvalues in the pseudocontinuous spectrum can be estimated as $\mu_1(\nu_0) = -\mathrm{Re}\left[\ln Y(\nu_0)\right]$. In particular, at $\nu_0 = 0$ we have two solutions

$$\mu_1 = \nu_1 = 0, \text{ and } \mu_1 = -\mathrm{Re}\left[\ln\left(\frac{1+e^{G_0}R}{1+R}\right)\right] < 0 \quad .$$

#189874 - $15.00 USD Received 7 May 2013; revised 27 Jun 2013; accepted 27 Jun 2013; published 6 Aug 2013

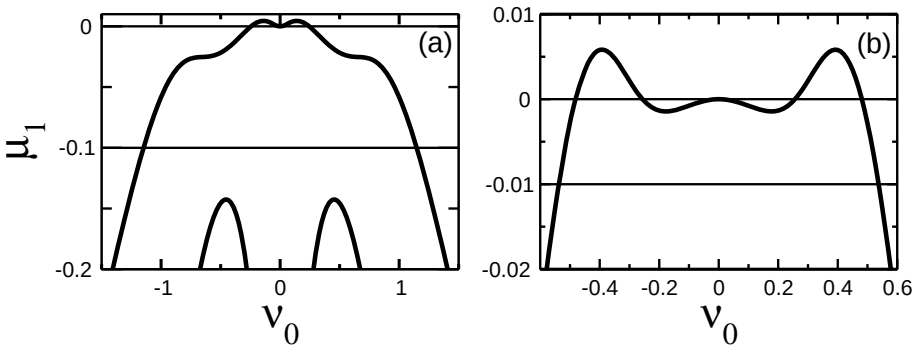


Fig. 6. Real parts of the eigenvalues of the CW solution vs their imaginary parts. Panels (a) and (b) illustrate modulational and Turing instabilities, respectively. The parameter values are the same as in Fig. 5.

The first of these solutions corresponds to the zero eigenvalue, $\lambda = 0$, related to the phase shift invariance of the model Eqs. (1) and (2) and the second to an eigenvalue with negative real part. In the limit $T \to \infty$ the zero eigenvalue gives rise to a branch $\mu_1(\nu_0)$ which is tangent to the imaginary axis $\mu_1 = 0$ at the point $\mu_1 = \nu_0 = 0$ of the $(\mu_1, \nu_0)$-plane (see Fig. 6).

The quasi-continuous branches shown in Fig. 6 are composed of a set of densely packed discrete eigenvalues with their imaginary parts behaving as $\nu_k \approx 2\pi k/T$ as $T \to \infty$ with $\nu_{k+1} - \nu_k = 2\pi/T$ equal to the spacing of the longitudinal cavity modes. In Fig. 6 (a) a modulational-like instability is shown where eigenvalues with small nonzero $k$-numbers, $0 < |k| < k_c$, where $k_c$ is come critical number, have crossed the imaginary axis. The instability of a given mode is associated with the growth of perturbations of the closest longitudinal modes. In Fig. 6 (b) a Turing-like instability is shown where eigenvalues with sufficiently large $k$-numbers centered around some $|k| = k_0$ acquire positive real parts.

A CW solution is modulationally unstable when the inequality $\frac{d^2\mu_1(0)}{d\nu_0^2} > 0$ holds, so that the zero eigenvalue is a local minimum of $\mu_1(\nu_0)$ at $\nu_0 = 0$. This condition can be rewritten in the form

$$[\alpha(\Delta - \omega) - 1]^2 < \frac{2\left(1+\alpha^2\right)\left(1+e^{G_0}R\right)(\Delta-\omega)^2}{(e^{G_0}-1)R}, \tag{11}$$

where $R$ and $\omega$ are defined by (4) and (5), respectively. It follows from this inequality that the mode at the filter centre frequency $\omega = \Delta$, is always stable with respect to modulational instability. With an increase of $|\omega - \Delta|$ a modulation instability of the the CW solution sets in (see Fig. 6(a)).

Table 1. Parameter values for simulations

| Parameter | Description | Value |
|---|---|---|
| $\gamma$ | Normalized carrier relaxation rate | 0.1 |
| $r$ | Normalized frequency sweep amplitude | 5 |
| $T$ | Normalized cavity round trip time | 200 |
| $\kappa$ | Linear attenuation factor | 0.2 |
| $\alpha$ | Linewidth enhancement factor | 2.0 |
| $g_0$ | Unsaturated gain per round trip | 3.0 |

#189874 - $15.00 USD Received 7 May 2013; revised 27 Jun 2013; accepted 27 Jun 2013; published 6 Aug 2013

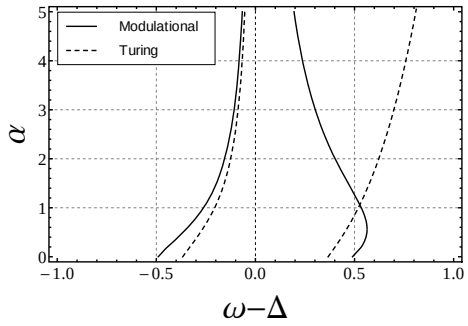


Fig. 7. Instability boundaries for the CW solutions. Solid and dashed lines show modulational and Turing instabilities, respectively. The parameter values are given in Tab. 1.

The boundaries of the modulational (Turing) instability are indicated by the solid (dashed) lines in Fig. 7. It is seen from this figure that depending on the parameter values and the sign of $\omega - \Delta$ the destabilization of the CW solution can take place either via a modulational instability or via a Turing instability. For zero $\alpha$ due to the symmetry of the model equations, the CW solution and its stability properties depend only on the absolute value $|\omega - \Delta|$. Thus, at $\alpha = 0$ the instability experienced by the CW regime is the same for both directions of the sweep of the filter central frequency $\Delta$. This symmetry is lost for sufficiently large values of $\alpha$ explaining the asymmetry of the experimentally observed time-traces with respect to the frequency sweep direction since typically SOAs such as that used in the experiment display an $\alpha$ greater than or approximately equal to 2. When the CW state is destabilized via a (long wavelength) modulational instability a transition to a complex and possibly chaotic, oscillating solution takes place, see Fig. 8. This suggests that the modulational instability is supercritical resulting in the creation of a stable oscillating solution from the destabilization of the CW regime. On the other hand, destabilization of the CW solution via the Turing instability results in a frequency jump to another CW solution with a frequency jump of the order of $2\pi k_0/T$. This suggests that the Turing instability is subcritical in the sense that any solution created from the destabilization of the CW mode is also unstable. A numerical simulation of the output is shown in Fig. 8. The simulation parameters are presented in Tab. 1.

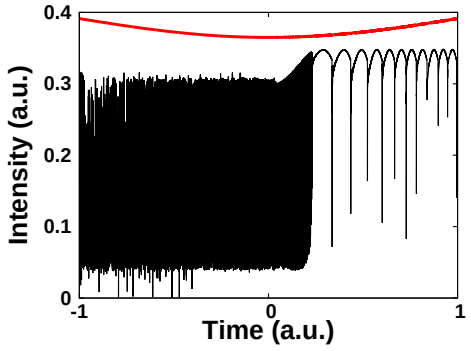


Fig. 8. Direct simulation of the model equations displaying the experimentally relevant asymmetry of the output intensity with respect to sweep direction. The parameter values are given in Tab. 1. The turning point of the modulation is at the 0 point of the x-axis and the sweeping voltage of the filter is shown (in red) above the intensity.

#189874 - $15.00 USD Received 7 May 2013; revised 27 Jun 2013; accepted 27 Jun 2013; published 6 Aug 2013

In the case when the central frequency of the filter is swept with a period close to the cavity round trip time one needs to use Eq. (8) with the term $\psi(t) = rT\frac{\varepsilon}{\Omega}\sin(\Omega t)$ in the exponential describing a slowly evolving phase accumulated due to the presence of a small frequency detuning $\varepsilon$ between the filter sweep rate and the inverse cavity round trip time ($\varepsilon = \Omega - 2\pi/T$). The form is precisely that of the quasistatic case and so, for sufficient detunings, the asymmetry must be preserved with abrupt frequency jumps arising from a Turing-like instability in one sweep direction and complex oscillations from a modulational instability in the other. However, because of the very different rates in the sine arguments, the asymmetry arises within one cavity round trip rather than over the long $\varepsilon^{-1}$ time scale of the quasistatic case. Furthermore, it is seen from Eqs. (8) and (9) that in the FDML case a change of the sign of the frequency sweep detuning $\varepsilon \to -\varepsilon$ is equivalent to a reversal of the frequency sweep direction. This explains the experimental result that the sweep direction asymmetry in the intensity traces is reversed when the detuning is changed from positive to negative.

## 5. Conclusions

To conclude, an analysis of the dynamics of an FDML laser is presented. Experimentally it was shown that an asymmetry in the output of an FDML source is observed, dependent on the sweep direction. When the frequency of the sweep is slightly greater than that of the cavity round trip the increasing wavelength part of the sweep results in a series of discrete frequency jumps while the decreasing wavelength part of the sweep results in a complex oscillating output. When the frequency of the sweep is slightly less than that of cavity round trip the asymmetry is reversed. Qualitatively similar results were found for a quasistatic regime and for a short cavity swept source. Further, the results were unchanged as the central wavelength of the optical spectrum was varied and so the phenomenon seems to be independent of cavity length and dispersion and thus most probably a result of the semiconductor carrier dynamics in the SOA. A mathematical model of an FDML laser based on a system of delay differential equations for the electric field envelope and carrier density in the semiconductor optical amplifier was proposed and analyzed analytically and numerically. We showed that the physics of the problem could be analyzed via the quasistatic regime by virtue of a transformation to a reference frame comoving with the filter. In particular a study of the evolution of the stability of the static CW solutions when undergoing an adiabatically slow sweep of the filter can explain the observations in the quasi-FDML regime. We showed that a modulational instability of the CW solution is responsible for the transitions to complex oscillating outputs and a Turing-type instability for the abrupt frequency jumps. Furthermore, this asymmetry is a consequence of the presence of a nonzero linewidth enhancement factor in the semiconductor optical amplifier. Finally, it is shown that slightly detuned FDML operation is formally equivalent to the quasistatic case but with the transitions between frequency swept FDML modes instead of the standard longitudinal laser modes. Our analysis explains also why the change of the sign of the frequency sweep detuning from the inverse cavity round trip time is equivalent to the reversal of the sweep direction.

## Acknowledgments

This work was conducted under the framework of the Irish Government's Programme for Research in Third Level Institutions Cycle 5, National Development Plan 2007-2013 via the INSPIRE programme with the assistance of the European Regional Development Fund. The authors also gratefully acknowledge the support of Science Foundation Ireland under Contract No. 11/PI/1152 and the EU FP7 Marie Curie Action FP7-PEOPLE-2010-ITN through the PROPHET project, Grant No. 264687. A.G.V. gratefully acknowledges the support of the Science Foundation Ireland E.T.S. Walton Visitors Award Programme under Contract No.

11/W.1/I2073 and SFB 787 of the DFG. The authors would like to acknowledge valuable discussions with Dr. Maciej Wojtkowski, D. Turaev and D. Rachinskii.

#189874 - $15.00 USD Received 7 May 2013; revised 27 Jun 2013; accepted 27 Jun 2013; published 6 Aug 2013